FULL PAPER

Self-Assembled Monolayer Coatings on Nanostencils for the Reduction of Materials Adhesion**

By *Marius Kölbel*, *R. Willem Tjerkstra*, *Gyuman Kim*, *Jürgen Brugger*, *Cees J. M. van Rijn*, *Wietze Nijdam*, *Jurriaan Huskens*,* and *David N. Reinhoudt**

Nanostencils (shadow masks with submicrometer apertures in a thin silicon nitride membrane) are promising tools for the facile one-step generation of nanopatterns of various materials by physical vapor deposition. Evaporation through a shadow mask is accompanied by gradual clogging of the apertures due to adhesion of evaporated material. In order to reduce this effect, nanostencils were coated with alkyl and perfluoroalkyl self-assembled monolayers (SAMs). The formation and properties of SAMs on planar silicon nitride substrates were studied by contact angle goniometry, X-ray photoelectron spectroscopy (XPS), and atomic force microscopy (AFM). The SAMs are stable under evaporation of gold at various angles. SAM-coated nanostencils showed considerably less adhesion of gold compared to bare Si_xN_y stencils.

1. Introduction

The spiraling progress information technology (IT) has seen over the last decades was essentially driven by ever faster hardware miniaturization. In the near future, however, the semiconductor industries will reach the resolution limits of optical lithography, their current central technology. These limitations on one hand, and the development of scanning probe techniques and nanotechnology in general on the other, have led to various novel patterning methods, e.g., electron beam lithography (EBL), focussed ion beam (FIB), X-ray lithography, soft lithography, and the nanostencil technique.[1]

A nanostencil consists of a thin silicon nitride membrane with aperture patterns obtained by optical lithography, EBL, or FIB, and is used as a shadow mask for the physical vapor deposition (PVD) of metals, semiconductors, insulators, or certain organic molecules onto various substrates under high vacuum (HV) or ultra-high vacuum (UHV) conditions. The fabrication of nanostencils with circular or line-shaped apertures having widths down to 200 nm is now state of the art, and further reduction of the aperture size down to 80 and 50 nm has been demonstrated.[1,2]

The principle of the nanostencil technique is shown in Figure 1. Shadow-mask evaporation technology has several advantages. It is a resistless technique that allows generation of patterns in a single step. Integration of an x,y-stage for substrates allows generation of a nearly unlimited number of patterns using a single mask. Employing a multi-material source, a broad variety of materials can be deposited within one processing step. The nanostencil technique allows fast and parallel replication of patterns in a way comparable to optical lithography. Expensive and low-throughput techniques such as EBL or FIB are necessary only for the fabrication of the nanostencil. Last but not least, the nanostencil technique is environmentally friendly, since no etchants and processing liquids are needed, and less waste is produced. In principle, evaporated feature sizes are limited only by the aperture sizes of the stencil and thus by the limitations in their fabrication.

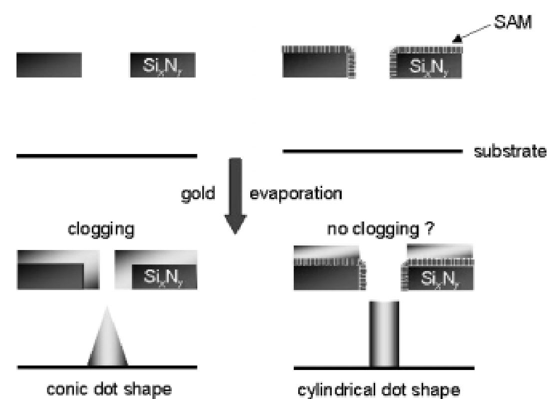

Fig. 1. Schematic representation of the nanostencil technique, the associated clogging problem, and the expected effect of SAM coatings.

The schematic representation of the formation of circular metal dots given in Figure 1 shows a potential problem which may occur when working with a nanostencil: evaporated mate-

[*] Dr. J. Huskens, Prof. D. N. Reinhoudt, Dr. M. Kölbel
Laboratory of Supramolecular Chemistry and Technology
MESA+ Research Institute, University of Twente
PO Box 217, NL-7500 AE Enschede (The Netherlands)
E-mail: smct@ct.utwente.nl; d.n.reinhoudt@ct.utwente.nl

Dr. R. W. Tjerkstra,
Transduction Technology Group
MESA+ Research Institute, University of Twente
PO Box 217, NL-7500 AE Enschede (The Netherlands)

Dr. G. Kim, Dr. J. Brugger[+]
NanoLink, MESA+ Research Institute, University of Twente
PO Box 217, NL-7500 AE Enschede (The Netherlands)

Dr. C. J. M. van Rijn, Dr. W. Nijdam,
Aquamarijn Micro Filtration B.V.
Beatrixlaan 2, NL-7255 DB Hengelo Gld. (The Netherlands)

[+] Present address: Microsystems Laboratory, École Polytechnique Fédérale de Lausanne, CH-1015 Lausanne, Switzerland.

[**] We thank Mark A. Smithers for SEM images, Albert van den Berg for XPS measurements and Frans Segerink for FIB experiments. The work was supported by the ATOMS project of the EU.

 © 2003 WILEY-VCH Verlag GmbH & Co. KGaA, Weinheim 1616-301X/03/0303-0219 $ 17.50+.50/0

rial is deposited not only on the substrate but also inside the apertures of the stencil, leading to their clogging.[1] Frequent cleaning of the nanostencil using etchants or plasma treatment may solve this problem, but is undesirable since it requires a time-consuming interruption of the HV process. Preventing adhesion of material to the aperture walls and thus increase of the performance and throughput of the nanostencil technique is envisaged by coating the nanostencil with an anti-adhesion layer. We chose to coat the nanostencils with organic self-assembled monolayers (SAMs) and to investigate their influence on the adhesion properties of the stencil. The SAMs are formed by an irreversible chemical surface reaction of silanes with surface OH groups.

2. SAMs on Silicon Nitride

Literature on the surface chemistry of silicon nitride is mainly limited to the functionalization of silicon nitride atomic force microscopy (AFM) tips and their interactions with various substrates. Although chemical modification of planar Si_xN_y surfaces with ω-alkenyl-, CH_3-, NH_2- and SO_3H-terminated monolayers has been reported in two articles on tip–sample interactions,[3] very few details on experimental conditions and monolayer stability that could be of potential value for our objective are given. Therefore we carried out some initial experiments on the formation of organic monolayers on Si_xN_y and studied their physical and chemical properties.[4]

Silicon nitride has a thin native SiO_2 coating layer, and its surface can be activated by treatment with piranha solution (H_2SO_4/30 % H_2O_2(aq), 3:1).[3] Afterwards, the surface is composed mainly of silanol and silazane groups.[5] Their ratio depends on various parameters, but at low pH and in the presence of water, mostly hydroxyl groups are found.[6] These surface groups react with silane or germane molecules to give the desired monolayers.

Whereas the self-assembly of thiols on gold surfaces yields highly ordered monolayers and can usually be easily reproduced, formation of monolayers on silicon oxide (as bulk material or as native oxide layer on Si or Si_xN_y) is less defined.[7] The silane (or germane) compounds used are usually trifunctional and react not only with surface OH groups but also with neighboring molecules in the monolayer. This cross-linking increases the stability of the layers. However, since the degree of cross-linking is influenced by various factors (temperature, water content), reproducibility is poor. In particular, water plays an important role in the surface reaction: traces of water appear to be necessary in order to hydrolyze the Si–Cl or Si–OR bonds of the silanes before the condensation reaction with surface OH groups can occur.[8] However, silanols generated by this hydrolysis can also react with chloro- or alkoxy silanes in solution, giving polymer threads and globules which can contaminate the surface by physisorption or chemisorption (via non-polymerized functionalities). Thus, working under exclusion of moisture is indispensable in order to avoid contamination and to suppress the competing bulk polymerization reactions, but complete removal of water from solvents, equipment, and substrates can inhibit the desired surface reaction. The optimal conditions for the reproducible formation of high quality monolayers must therefore be established by a trial-and-error approach.

Reproducible and good-quality SAMs were obtained by immersion of freshly cleaned Si_xN_y substrates in 0.2 vol.-% solutions of the silanes or germanes (for compounds see Table 1) in dry CH_2Cl_2 at room temperature over a period of 16 h, followed by extensive rinsing with organic solvents in order to remove physisorbed material. Compounds C12–$SiCl_3$ and CF–$SiMe_2Cl$ (because of its lower boiling point compared to CF–$Si(OEt)_3$) were employed in an attempt to carry out vapor phase formation of a SAM. The resulting monolayers were studied by dynamic contact angle goniometry (Table 1), tapping-mode AFM, and X-ray photoelectron spectroscopy (XPS). Ellipsometry was attempted but appeared to be useless because of the basically trilayer (Si/SiN/SAM) structure of the coated substrates; small errors in the estimated SiN thickness caused errors in the determination of the SAM thickness larger than the SAM itself.

Table 1. Dynamic advancing and receding water contact angles for silane and germane SAMs on Si_xN_y.

		θ_{adv} [°]	θ_{rec} [°]
C12-SiCl$_3$	$Cl-SiCl_2-C_{12}H_{25}$	115 118 [a]	91 84 [a]
C12-Si(OEt)$_3$	$EtO-Si(OEt)_2-C_{12}H_{25}$	113	93
CF-Si(OEt)$_3$	$EtO-Si(OEt)_2-CH_2CH_2-C_8F_{17}$	120	95
CF-SiMe$_2$Cl	$Cl-Si(CH_3)_2-CH_2CH_2-C_8F_{17}$	113 [a]	88 [a]
HOOC-GeCl$_3$	$Cl-GeCl_2-CH_2CH_2-COOH$	<20	<20

[a] Deposition from the gas phase.

The water contact-angle data indicate hydrophobic surfaces with a hysteresis of 20–25° for the alkyl and perfluoroalkyl SAMs deposited from solution. This is in accordance with values reported for silane SAMs on silicon oxide.[9] Also the higher hydrophobicity of perfluorinated SAMs compared to hydrocarbon SAMs has been observed before.[10] For CF–$SiMe_2Cl$, a slightly less hydrophobic and less ordered SAM compared to CF–$Si(OEt)_3$ was observed. This is ascribed to a lower surface density of perfluoroalkyl chains due to the space required by the methyl groups. Nevertheless, the difference in SAM quality is small (also for C12–$SiCl_3$) and gas phase deposition can thus be regarded as a valuable, alternative preparation method

© 2003 WILEY-VCH Verlag GmbH & Co. KGaA, Weinheim

equivalent to solution deposition. The reduced demand of solvents and the exclusion of solution polymerization may make it preferable for some applications from a technical point of view. The low contact angle values measured for the SAM of the trichlorogermane HOOC–$GeCl_3$ indicate successful formation of a closely packed, highly hydrophilic SAM.

AFM showed smooth surfaces with very few thread-like or globular aggregates (height ~5 nm), most likely resulting from some solution polymerization. The roughness is comparable to that of bare silicon nitride surfaces (root-mean-square (RMS) roughness over 100 μm^2 for bare Si_xN_y is 0.66 nm, for C12–$Si(OEt)_3$-SAM 0.83 nm).

Despite the XPS penetration depth of only 5 nm, intense signals for Si and N were observed which can be ascribed to the Si_xN_y substrate. This confirms the absence of multilayers, as a monolayer has a thickness of ~2 nm. The atomic concentrations of C and/or F are in the expected range, although somewhat obscured by excess carbon, probably from atmospheric contamination.[11]

Since we chose the apolar compounds C12–$SiCl_3$, C12–$Si(OEt)_3$, and CF–$Si(OEt_3)$ for coating the nanostencils, we also carried out experiments on their chemical and physical stability. We found (based on contact-angle measurements) that these monolayers can be stored at ambient conditions for months without changes in their properties. They are stable against repeated washings with organic solvents like CH_2Cl_2, ethanol, hexane, and toluene. No change in contact angles was detected after 24 h immersion in water and after storing the samples in an oven at 100 °C for 2 h. In basic cyanide gold etch solution the contact angle did not decrease for immersion times of up to 10 min. Surprisingly, the SAMs are also relatively stable in piranha solution. The advancing water contact angle decreased $< 5°$ over 1 h for CF–$Si(OEt)_3$ and ~10° over 1 h for C12–$SiCl_3$. The receding contact angles decreased by 10–15° for both SAMs.

In order to check the stability of the SAMs under the conditions of metal evaporation we carried out an experiment with evaporation followed by etching (Fig. 2). In this experiment, SAMs of C12–$SiCl_3$ and CF–$Si(OEt)_3$ were prepared on silicon nitride substrates. The advancing and receding water contact angles were found to be as listed in Table 1. One half of the substrate was masked with a silicon square. Then 40 nm gold was evaporated onto the unprotected region under an angle of 90°. The evaporation was carried out using a thermal evaporator. The change in thickness of the gold layer formed was monitored by means of an internal quartz crystal microbalance (QCM). After this process, the contact angles of the uncoated region of the monolayer had not changed significantly, whereas the gold-coated area showed strongly reduced hydrophobicity. The gold was removed by selective etching ($K_3[Fe(CN)_6]$/$K_4[Fe(CN)_6]$/KOH/$Na_2S_2O_3$, 15 min). Hereafter, the advancing contact angle was about ~12° lower on both areas. This change can probably be ascribed to the etch process. The absence of a difference between gold-covered and uncovered areas led us to conclude that bombardment with gold under HV conditions has no destructive impact on an alkylsilane or perfluoroalkylsilane monolayer. The slight damage to the SAM apparently caused by the etchant convinced us to use I_2/KI etch solution in further experiments. SAMs on planar Si_xN_y substrates were found to be stable in this etchant without significant changes in contact angles for immersion times of at least 1 h.

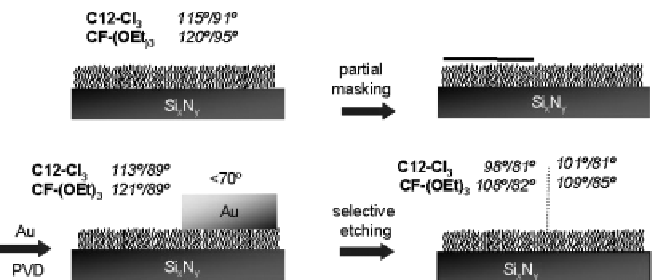

Fig. 2. Experiment on bombardment of SAMs with high-energy gold atoms; advancing/receding dynamic water contact angles for SAMs of C12–$SiCl_3$ and CF–$Si(OEt)_3$ after individual steps of the procedure.

In order to better model evaporation inside the apertures, planar substrates with and without CF–$Si(OEt)_3$ SAM were placed at angles of 45°, 30°, and 0° with the direction of the incoming gold. The last case represents lateral bombardment of the SAM, with the high-energy metal atoms attacking the molecules in the SAM, not at their end, but perpendicular to their chain, as is likely to be the case in the nanostencil apertures. After evaporation of 40 nm gold, the substrates placed at angles of 45° and 30° were covered with a layer of gold visible to the naked eye, for the SAM-coated substrates as well as for the untreated controls. For the substrates placed at 0°, however, no gold deposition was apparent. Water contact angle measurements at the SAM-coated sample showed no decrease in hydrophobicity ($\theta_{adv} = 120°$), but no distinct value for the receding contact angle could be measured, indicating that the order of the SAM had somewhat decreased. The latter observation can be ascribed to adhesion of small amounts of gold to the SAM-coated surface (3 % according to XPS measurements). These results indicate that the SAMs are also stable under lateral bombardment.

3. Experiments with Nanostencils

The nanostencils used were made by silicon micromachining as shown in Figure 3. They consist of silicon nitride membranes with hexagonal arrays of holes having nominal diameters of 500 nm, and spacings of 1 μm. The thickness of the membranes is 800 nm. The holes have a tapered cross-section. Whereas on one side their diameters correspond to the nominal value, they are 605 ± 35 nm on the other side (Fig. 4).

The SAM coating of the nanostencils was carried out in exactly the same manner as described above for planar substrates. In order to be able to clearly visualize differences in material deposition inside the stencil apertures, large amounts of gold (thickness 1 μm) were evaporated. The setup is shown in Figure 5. The nanostencils were placed on silicon substrates (1 cm × 1 cm). The face with the smaller aperture diameters was positioned towards the gold source, the opposite face to-

© 2003 WILEY-VCH Verlag GmbH & Co. KGaA, Weinheim
1616-301X/03/0303-0221 $ 17.50+.50/0

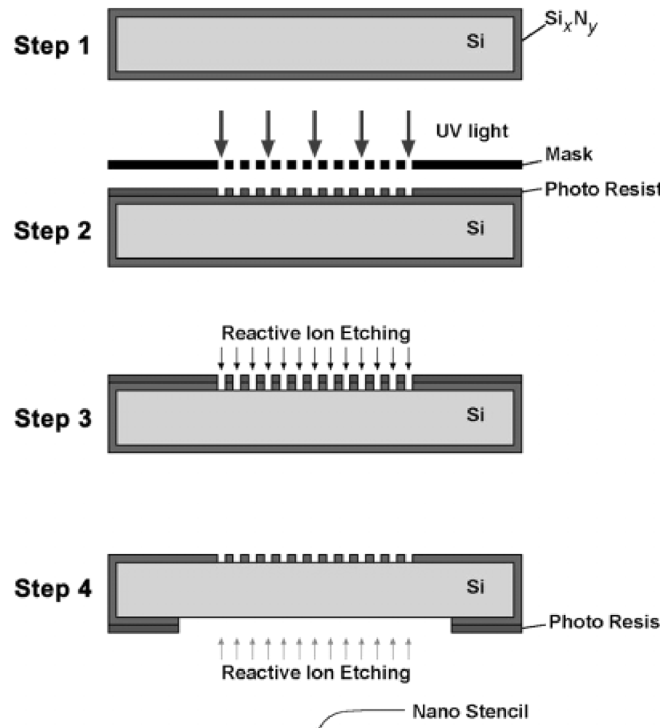

Fig. 3. Fabrication of the nanostencil.

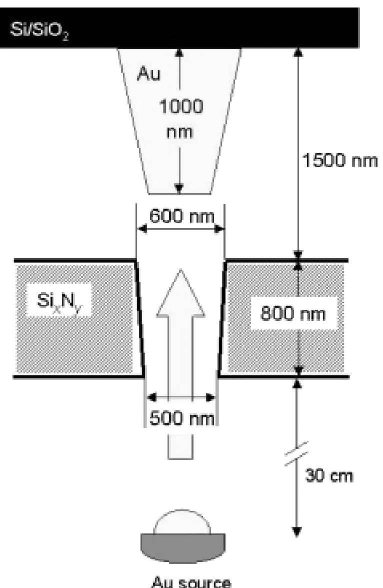

Fig. 4. Geometrical parameters of the nanostencils and the evaporation process.

wards the substrate. In order to prevent the micrometer dots from growing into the stencil apertures, a photoresist spacer ring of 1.5 μm height was fabricated on the substrate. A flexible metal clamp was used to hold the samples in place on a sample holder, an aluminum plate with a diameter of 3 in. (1 inch = 2.54 cm) with windows for the samples.

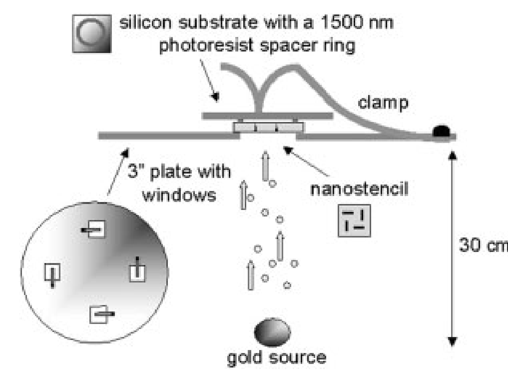

Fig. 5. Experimental setup for nanostencil evaporation experiments.

After the evaporations, the nanostencils were investigated by scanning electron microscopy (SEM). FIB etching was used to cut slits into the gold-covered membranes in order to image the cross-sections of the apertures by FIB itself (not shown) and by SEM under high tilt angles.[12]

Figure 6 shows SEM images of the nanostencil after evaporation of 1 μm gold through 500 nm apertures. Clearly, the

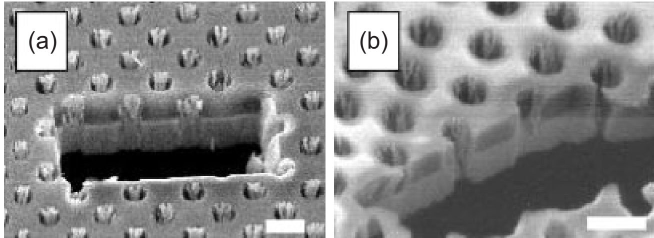

Fig. 6. SEM images of stencils after evaporation of 1 μm Au. a**)** Uncoated (15 300 ×), b) CF–Si(OEt)$_3$ coated (22 000 ×); scale bars: 1 μm.

holes of the untreated nanostencil contain more gold than those of the CF–Si(OEt)$_3$ coated stencils. The pictures show that the gold forms long, leaf-shaped deposits in the holes of the former, indicating diffusion controlled growth, whereas only thin lines of gold are deposited inside the CF–Si(OEt)$_3$ coated apertures. The same difference with uncoated nanostencils was observed for the evaporation of 1 μm gold through 500 nm apertures coated with C12–Si(OEt)$_3$.[13]

The improved sticking properties of the coated stencils prove that SAM formation has taken place inside the apertures as well as on the planar areas. The highly apolar monolayers strongly reduce the attractive interactions of the nanostencil surface with gold. Obviously, at the macroscopic outer surface, deposition does occur in any case because the gold hits the surface. In the nanoscopic pores, however, under the parallel flow of gold atoms, the reduced sticking appears to prevent the formation of gold clusters early in the process which can act as nucleation centers for the rapid growth of crystalline gold. This gold deposition inside the pores does, however, occur for the uncoated samples. Also, we observed that gold peels off easier from the SAM-coated stencils than from the uncoated ones.

 © 2003 WILEY-VCH Verlag GmbH & Co. KGaA, Weinheim 1616-301X/03/0303-0222 $ 17.50+.50/0

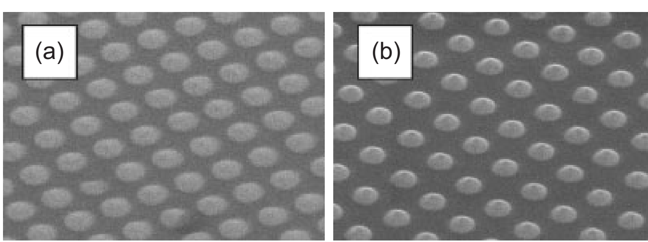

Fig. 7. SEM images of dot patterns formed following the evaporation of 150 nm Au through a) uncoated, and b) CF–Si(OEt)$_3$-coated nanostencils with 350 nm pore diameters and a 1 μm pitch.

Some evaporation results are shown in Figure 7, which shows SEM images of substrates after the evaporation of 150 nm of gold through such nanostencils, either uncoated (a) or coated with a CF–Si(OEt)$_3$ monolayer (b). The patterns for the uncoated stencil are clearly less well-defined and cover larger areas than patterns obtained with the coated stencil. More quantitative AFM analyses show almost a nominal height for patterns obtained with the coated stencil (147 nm), while a height of only 65 nm is observed for the patterns obtained with the uncoated stencil. Also the total dot volume appears to be a factor of two to three higher for coated stencils. A more quantitative description of the resulting patterns will be given elsewhere.[14]

Evaporation of material through the nanostencils inevitably leads to deposition on top of the nanostencil. This is particularly visible in Figure 6, which shows nanostencils after evaporation of 1 μm of gold. This figure also shows that with such high loadings (or after repeated evaporations with a comparable total amount) the pores inside the built-up gold are smaller than the original stencil apertures. The consequences of this for the resulting patterns for such large evaporation amounts will be described elsewhere.[14] Nevertheless, these results clearly show that cleaning is necessary after evaporating such amounts before re-use of the same nanostencils. The nanostencils could be cleaned easily by immersion in I_2/KI gold etch solution (0.2 g I_2, 3.15 g KI in 50 mL H_2O) for ~10–20 min at room temperature. As mentioned earlier, the SAMs are stable under these conditions. No difference in etch rate between coated and uncoated nanostencils was observed.

4. Conclusions

We were able to show that silane SAMs on silicon nitride can be prepared and have properties comparable to those known from SAMs on silicon dioxide. The SAMs are stable against various physical and chemical influences and against vertical and lateral bombardment with gold vapor in HV. SAM coatings were expected to reduce adhesion of gold inside the apertures of silicon nitride nanostencil membranes. This effect is confirmed by SEM on nanostencils after gold evaporation: the images clearly show that less gold is deposited inside the pores of SAM-coated stencils compared to uncoated ones. These results show that SAM coatings can be used to improve performance and lifetime of nanostencils, thus increasing the throughput of this promising new nanopatterning technique.

5. Experimental

Chemicals and Instrumentation: Dodecyltrichlorosilane was purchased from Aldrich, dodecyltriethoxysilane and carboxyethyltrichlorogermane from ABCR, 1*H*,1*H*,2*H*,2*H*-perfluorodecyltriethoxysilane and 1*H*,1*H*,2*H*,2*H*-perfluorodecyldimethyltrichlorosilane from Lancaster. All compounds were used as obtained. Contact angles were determined using a Krüss Contact Angle Measurement System G10, and the data processed with the program Drop Shape Analysis 1.51. SEM images were taken with a Hitachi S800 FEG-SEM. A PHI Quantum 2000 scanning X-ray microprobe was employed for XPS investigations. FIB experiments were carried out by means of a FIB 200 (FEI Company).

Nanostencil Fabrication: The nanostencils used were made by silicon micromachining as shown in Figure 3. A thin layer (thickness 500 nm) of low stress silicon nitride was deposited on a one side polished Si⟨100⟩ wafer by Low Pressure Chemical Vapor Deposition (SiH_2Cl_2/NH_3 = 70:18 at 850 °C, 250 mbar) (step 1). A pattern with 500 nm pores in photo resist was made using mask photolithography (wafer stepper ASML PAS 5000/50) on the polished side of the silicon nitride (step 2). After development, this pattern was etched using reactive ion etching (CHF_3/O_2 = 25:5, power = 75 W, pressure = 10 mbar, 6 min) creating pores in the silicon nitride (step 3). In step 4, the process of lithography and reactive ion etching was repeated on the back side of the wafer, defining large rectangular openings in the silicon nitride. The silicon between the nanostencil layer and the back side was removed in an anisotropic etch step along the Si⟨111⟩ planes with a 25 % KOH solution at 70 °C until the membrane layer was reached (step 5). The nanostencils were diced at a rate of 2 mm s^{-1} (to avoid damage of the nanostencil) into square pieces of 5 mm × 5 mm and cleaned in a 25 % KOH (70 °C) and a 5 % H_2SO_4 solution (40 °C) to remove all silicon particles that were released during dicing.

SAM Formation: All glassware was immersed in fresh piranha solution of ~80 °C for at least 1 h, rinsed three times with milliQ water, blown dry with nitrogen, and stored in a glove box under N_2 (not longer than 2 h). The planar silicon nitride substrates (150 nm Si_xN_y on Si, 1 cm × 1 cm) or nanostencils were treated with fresh piranha solution for 30 min, rinsed three times with milliQ water, blown dry with nitrogen, and also stored in a glove box under N_2 prior to use (not longer than 1 h). Solutions were prepared immediately before use. 0.05 mL silane or germane were added to 25 mL CH_2Cl_2 (freshly distilled from $CaCl_2$) in a glass dish inside the glovebox. The substrates were immersed in the solution and the dish covered with a lid. After 16 h the substrates were transferred into a beaker containing 20 mL distilled CH_2Cl_2 and rinsed under shaking. The solvent was discarded and the rinsing repeated three times. After addition of another 20 mL CH_2Cl_2, the substrates were taken out of the glovebox and rinsed again with two 20 mL portions of CH_2Cl_2, absolute EtOH, and CH_2Cl_2. The substrates were then blown dry with N_2. For gas phase deposition, the piranha-cleaned substrate was placed top-down above a dish containing 1 mL silane in a dessicator. The dessicator was evacuated to ~10 mbar, and after standing for 16 h at room temperature the substrate was removed and treated in the same manner as described for solution deposition.

Evaporations: The sample holder was placed in a Balzers BA 510 thermal evaporator, 30 cm above and at an angle of ~5° to the evaporation source. The chamber was evacuated to ~5×10^{-6} mbar before the evaporation was started. The pressure during evaporation was ~5×10^{-5} mbar, the voltage 90 V, the evaporation rate ~24 nm min^{-1}. The change in thickness of the gold layer formed was monitored by means of an internal quartz crystal microbalance (QCM).

Cleaning of the Stencils: The nanostencils were immersed in a solution of 0.2 g I_2 and 3.15 g KI in 50 mL H_2O. The progress of the etching reaction was monitored in intervals of 5 min by optical microscopy after rinsing with milliQ water and drying the stencils in an N_2 stream. 20 min was sufficient for complete removal of the gold.

Received: May 6, 2002
Final version: September 6, 2002

[1] a) R. Lüthi, R. R. Schlittler, J. Brugger, P. Vettiger, M. E. Welland, J. K. Gimzewski, *Appl. Phys. Lett.* **1999**, *75*, 1314. b) J. Brugger, J. W. Berenschot, S. Kuiper, W. Nijdam, B. Otter, M. Elwenspoek, *Microelectron. Eng.* **2000**, *53*, 403. c) M. M. Deshmukh, D. C. Ralph, M. Thomas, J. Silcox, *Appl. Phys. Lett.* **1999**, *75*, 1631. d) R. R. Schlittler, J. W. Seo, J. K. Gimzewski, C. Durkan, M. S. M. Saifullah, M. E. Welland, *Science* **2001**, *292*, 1136.

[2] C. J. M. van Rijn, G. J. Veldhuis, S. Kuiper, *Nanotechnology* **1998**, *9*, 343.

[3] a) T. Ito, M. Namba, P. Bühlmann, Y. Umezawa, *Langmuir* **1997**, *13*, 4323. b) V. V. Tsukruk, V. N. Bliznyuk, *Langmuir* **1998**, *14*, 446.

[4] M. Kölbel, J. Huskens, J. Brugger, D. N. Reinhoudt, *Proc. Micro Nano Eng. Conf. 2001*, Grenoble, September, **2001**, p. 350.

[5] G. Busca, V. Lorenzelli, M. I. Braton, R. Marchand, *J. Mol. Struct.* **1986**, *143*, 525.

 © 2003 WILEY-VCH Verlag GmbH & Co. KGaA, Weinheim 1616-301X/03/0303-0223 $ 17.50+.50/0

[6] a) L. Bergström, E. Bostedt, *Colloids Surf.* **1990**, *49*, 183. b) M. Okabe, S. Okazi, *Nippon Kagaku Kaishi* **1989**, *10*, 1802. c) Y. Li, Y. Gao, Y. Liang, F. Zheng, K. Xiao, Z. Hu, *Wuli Huaxue Xuebao* **1995**, *11*, 886.
[7] A. Ulman, *Chem. Rev.* **1996**, *96*, 1533.
[8] M. E. McGovern, K. M. R. Kallury, M. Thompson, *Langmuir* **1994**, *10*, 3607.
[9] A. Ulman, *An Introduction to Ultrathin Organic Films,* Academic Press, Boston, MA **1991**.
[10] M.-W. Tsao, J. F. Rabolt, H. Schönherr, D. G. Castner, *Langmuir* **2000**, *16*, 1734.
[11] The atomic concentration of C in Si_xN_y substrates when measured without pre-treatment was up to 40 %. XPS, carried out after 30 min cleaning in piranha solution, still gives ~ 8 % C.
[12] FIB cross-sections did not give reliable information since it was difficult to distinguish between gold deposited during the PVD process and gold re-deposited during the FIB etching. Our conclusions are based exclusively on SEM images of apertures to which no FIB had been applied.
[13] C12–$Si(OEt)_3$ and C12–$SiCl_3$ give SAMs with nearly identical properties. The results obtained with C12–$SiCl_3$ on stencils are, however, less reproducible. We assume this to be due to the higher reactivity and moisture sensitivity of the compound compared with C12–$Si(OEt)_3$ and recommend always the use of alkoxy silanes.
[14] M. Kölbel, R. W. Tjerkstra, J. Brugger, C. J. M. van Rijn, W. Nijdam, J. Huskens, D. N. Reinhoudt, *Nano Lett.* **2002**, *2*, 1339.

 © 2003 WILEY-VCH Verlag GmbH & Co. KGaA, Weinheim 1616-301X/03/0303-0224 $ 17.50+.50/0